

# Journal of Astronomical Telescopes, Instruments, and Systems

AstronomicalTelescopes.SPIEDigitalLibrary.org

## **Porous plug phase separator and superfluid film flow suppression system for the soft x-ray spectrometer onboard Hitomi**

Yuichiro Ezoe  
Michael DiPirro  
Ryuichi Fujimoto  
Kumi Ishikawa  
Yoshitaka Ishisaki  
Kenichi Kanao  
Mark Kimball  
Kazuhisa Mitsuda  
Ikuyuki Mitsuishi  
Masahide Murakami  
Hirofumi Noda  
Takaya Ohashi  
Atsushi Okamoto  
Yohichi Satoh  
Kosuke Sato  
Peter Shirron  
Shoji Tsunematsu  
Hiroya Yamaguchi  
Seiji Yoshida

Yuichiro Ezoe, Michael DiPirro, Ryuichi Fujimoto, Kumi Ishikawa, Yoshitaka Ishisaki, Kenichi Kanao, Mark Kimball, Kazuhisa Mitsuda, Ikuyuki Mitsuishi, Masahide Murakami, Hirofumi Noda, Takaya Ohashi, Atsushi Okamoto, Yohichi Satoh, Kosuke Sato, Peter Shirron, Shoji Tsunematsu, Hiroya Yamaguchi, Seiji Yoshida, "Porous plug phase separator and superfluid film flow suppression system for the soft x-ray spectrometer onboard Hitomi," *J. Astron. Telesc. Instrum. Syst.* **4**(1), 011203 (2017), doi: 10.1117/1.JATIS.4.1.011203.

# Porous plug phase separator and superfluid film flow suppression system for the soft x-ray spectrometer onboard Hitomi

Yuichiro Ezoe,<sup>a,\*</sup> Michael DiPirro,<sup>b</sup> Ryuichi Fujimoto,<sup>c</sup> Kumi Ishikawa,<sup>d</sup> Yoshitaka Ishisaki,<sup>a</sup> Kenichi Kanao,<sup>e</sup> Mark Kimball,<sup>b</sup> Kazuhisa Mitsuda,<sup>d</sup> Ikuyuki Mitsuishi,<sup>f</sup> Masahide Murakami,<sup>g</sup> Hirofumi Noda,<sup>h</sup> Takaya Ohashi,<sup>a</sup> Atsushi Okamoto,<sup>i</sup> Yohichi Satoh,<sup>i</sup> Kosuke Sato,<sup>j</sup> Peter Shirron,<sup>b</sup> Shoji Tsunematsu,<sup>e</sup> Hiroya Yamaguchi,<sup>b</sup> and Seiji Yoshida<sup>d</sup>

<sup>a</sup>Tokyo Metropolitan University, Department of Physics, Hachioji, Tokyo, Japan

<sup>b</sup>National Aeronautics and Space Administration, Goddard Space Flight Center, Greenbelt, Maryland, United States

<sup>c</sup>Kanazawa University, Institute of Science and Engineering, Faculty of Mathematics and Physics, Kakuma-machi, Kanazawa, Ishikawa, Japan

<sup>d</sup>Japan Aerospace and Exploration Agency, Institute of Space and Astronautical Science, Sagami-hara, Kanagawa, Japan

<sup>e</sup>Sumitomo Heavy Industries, Ltd., Niihama, Ehime, Japan

<sup>f</sup>Nagoya University, Department of Physics, Chikusa-ku, Nagoya, Japan

<sup>g</sup>University of Tsukuba, Department of Engineering Mechanics and Energy, Tsukuba, Ibaraki, Japan

<sup>h</sup>Tohoku University, Frontier Research Institute for Interdisciplinary Sciences, Aoba, Sendai, Japan

<sup>i</sup>Japan Aerospace Exploration Agency, Research and Development Directorate, Tsukuba, Ibaraki, Japan

<sup>j</sup>Tokyo University of Science, Department of Physics, Tokyo, Japan

**Abstract.** When using superfluid helium in low-gravity environments, porous plug phase separators are commonly used to vent boil-off gas while confining the bulk liquid to the tank. Invariably, there is a flow of superfluid film from the perimeter of the porous plug down the vent line. For the soft x-ray spectrometer onboard ASTRO-H (Hitomi), its approximately 30-liter helium supply has a lifetime requirement of more than 3 years. A nominal vent rate is estimated as  $\sim 30 \mu\text{g/s}$ , equivalent to  $\sim 0.7 \text{ mW}$  heat load. It is, therefore, critical to suppress any film flow whose evaporation would not provide direct cooling of the remaining liquid helium. That is, the porous plug vent system must be designed to both minimize film flow and to ensure maximum extraction of latent heat from the film. The design goal for Hitomi is to reduce the film flow losses to  $< 2 \mu\text{g/s}$ , corresponding to a loss of cooling capacity of  $< 40 \mu\text{W}$ . The design adopts the same general design as implemented for Astro-E and E2, using a vent system composed of a porous plug, combined with an orifice, a heat exchanger, and knife-edge devices. Design, on-ground testing results, and in-orbit performance are described. © The Authors. Published by SPIE under a Creative Commons Attribution 3.0 Unported License. Distribution or reproduction of this work in whole or in part requires full attribution of the original publication, including its DOI. [DOI: [10.1117/1.JATIS.4.1.011203](https://doi.org/10.1117/1.JATIS.4.1.011203)]

Keywords: ASTRO-H (Hitomi); soft x-ray spectrometer; x-ray microcalorimeter; cryogenics; superfluid helium; porous plug; film flow. Paper 17016SSP received Apr. 20, 2017; accepted for publication Oct. 3, 2017; published online Oct. 27, 2017.

## 1 Introduction

ASTRO-H (Hitomi)<sup>1</sup> is the sixth Japanese x-ray astronomy satellite. It was launched on February 17, 2016, and was decommissioned due to loss of the attitude control on March 26, 2016. The soft x-ray spectrometer (SXS)<sup>2</sup> onboard Hitomi is an x-ray microcalorimeter operated at 50 mK, providing a nondispersive energy resolution of  $< 7 \text{ eV}$  (full width at half maximum) in the 0.3- to 12-keV bandpass. The microcalorimeter is cooled down from room temperature to 50 mK using a dewar, four 2-stage Stirling cryocoolers, a Joule–Thomson cryocooler, superfluid helium-4, and a 3-stage adiabatic demagnetization refrigerator (ADR).<sup>3,4</sup> Although the SXS was still in the commissioning phase, it had successfully shown the superb energy resolution on-orbit and provided valuable data sets from aspects of both science and engineering.<sup>2</sup>

At nominal operation, an average heat load on the helium tank is  $\sim 0.7 \text{ mW}$ .<sup>3–5</sup> Assuming this heat load and an initial fill level of 30 L, the lifetime of the helium will be  $\sim 4$  years. As shown in Table 1, this heat load is lower than any previous

space missions using superfluid helium, even compared to values of the two previous x-ray microcalorimeter instruments, the ASTRO-E XRS and the Suzaku XRS2. These two missions planned astronomical observations but were lost due to a rocket failure and a boil-off of the entire liquid helium, respectively. With SXS, we succeeded in conducting the first astronomical observations by an orbiting x-ray microcalorimeter.

To safely vent the small helium gas flow and suppress a superfluid film flow, we employed a porous plug phase separator and a film flow suppression system. The superfluid film flow can lead to a potential loss of the superfluid helium, because the average heat load is tiny. In this paper, we describe design and performance of the porous plug and superfluid film flow suppression system for the SXS.

## 2 Design

### 2.1 Overview

The porous plug phase separator and the film flow suppression system are designed based on ASTRO-E XRS and Suzaku XRS2 heritages.<sup>14</sup> It consists of four devices as shown in Fig. 1. The design of the system is described in Ref. 15.

\*Address all correspondence to: Yuichiro Ezoe, E-mail: [ezoe@tmu.ac.jp](mailto:ezoe@tmu.ac.jp)

**Table 1** Past space missions using superfluid helium-4.

Mission	Volume (L)	Helium lifetime (months)	Average heat load (mW)	References
IRAS	560	10	71	6
COBE	660	10	83	7
ISO	2300	28	110	8
GP-B	2500	17	190	9
Akari	170	12	10	10
Spitzer	360	68	6.2	6
ASTRO-E XRS	30	23 (predicted) <sup>a</sup>	0.96	11 and 12
Suzaku XRS2	30	36 (predicted)	0.93	13

<sup>a</sup>The XRS used solid neon as 17-K heat bath. The lifetime of solid neon is shorter than that of superfluid helium. The superfluid helium would go away after the loss of the solid neon. Thus, we here describe the lifetime of solid neon.

Ground tests of bread board model, engineering model, and flight model (FM) systems are described in Refs. 16–19. The design is explained below.

Under zero gravity, a simple vent hole on the top of the tank would not work because the liquid is not always at the bottom. The role of the porous plug is to let helium gas out while retaining superfluid liquid helium in the tank.

At the same time, a small amount of superfluid film flow out of the vent line could influence the helium lifetime, since the gas flow rate is so small. To reduce the film flow, three devices, an orifice, a heat exchanger, and knife-edge devices are included. Without this film flow suppression system, the film flow rate would be  $\sim 50 \mu\text{g/s}$ , corresponding to an effective cooling loss of  $\sim 1 \text{ mW}$ .

Requirements for the porous plug and the film flow suppression system are summarized in Table 2. The SXS planned to observe astronomical objects for 3 years with a goal of 5 years. Assuming 30-L superfluid helium, a 5-year lifetime gives an average heat load on the helium tank of 0.59 mW and an average helium flow rate of  $28 \mu\text{g/s}$ . The expected helium tank temperature was 1.15 K. Mass flow rates at the beginning and the end of life estimated by the thermal analysis are 33 and  $43 \mu\text{g/s}$ , respectively. Considering uncertainties of the thermal analysis and safety margin, we required the mass flow rate of  $28 \mu\text{g/s}$  at 1.15 K. The film flow rate must be  $< 2 \mu\text{g/s}$ , to avoid an additional loss of helium.

Two off-nominal cases must be taken into account. In the single cryocooler failure case, we assume that one of the four cryocoolers stops, which results in an increase of the heat load on the helium tank. In this case, the tank temperature should be kept below 1.50 K for the ADR efficiency. Thus, the mass flow rate of  $86 \mu\text{g/s}$  larger than the nominal case must be safely vented at the helium tank temperature of  $< 1.50 \text{ K}$ .

In the no cryocoolers case, all the cryocoolers are temporarily off (e.g., just after launch). If this situation continues for an unexpected long time, the heat load on the helium tank can reach 73 mW, corresponding to the mass flow rate of  $3200 \mu\text{g/s}$ . Even in such an emergency situation, the helium tank should be

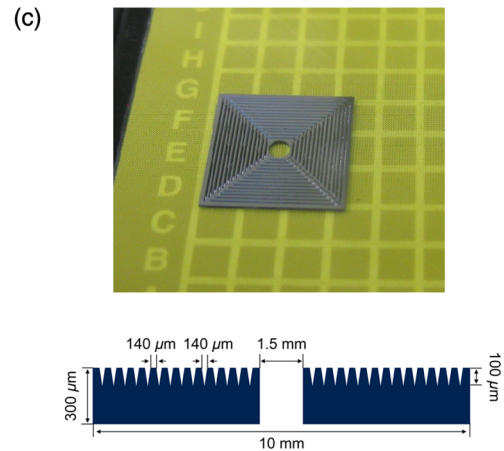
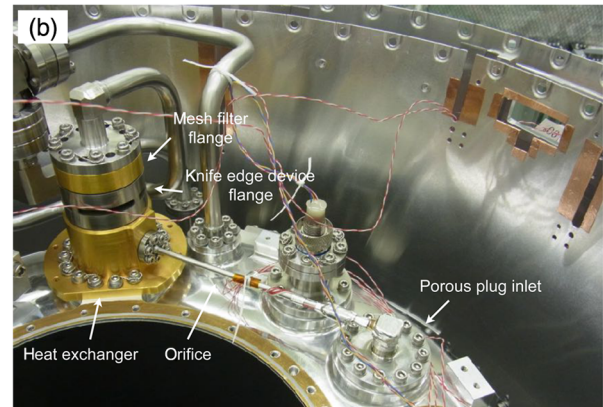
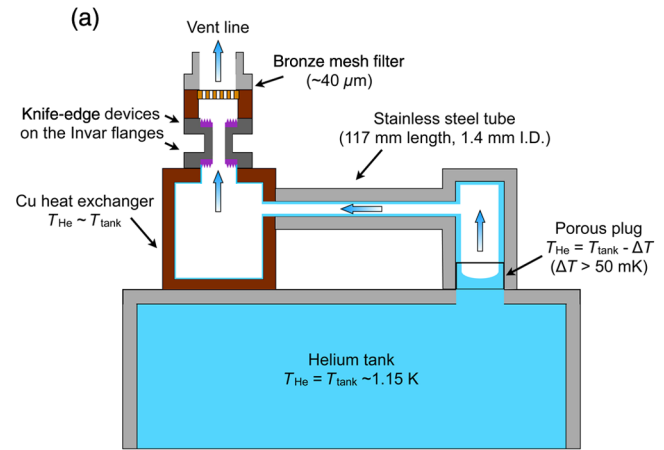


**Fig. 1** (a) Schematic view of the porous plug and film flow suppression system. (b) Photo of the FM system installed in the dewar. (c) Photo of a knife-edge device and its cross-sectional view. Figures are taken from Ezoe et al.<sup>19</sup>

kept below  $\lambda$  point ( $\sim 2.15 \text{ K}$ ) with some margin ( $\sim 0.1 \text{ K}$ ), to keep superfluid helium in the tank.

We have designed and tested the whole system, to satisfy all the requirements. The principles and design of the four components are as follows.

## 2.2 Porous Plug

A porous plug is a traditional device to separate helium gas from superfluid helium in zero gravity using the thermomechanical

**Table 2** Requirements for the SXS porous plug and film flow suppression system.<sup>19</sup>

Case	Nominal <sup>a</sup>	Single cryocooler failure	No cryocoolers
Heat load (mW)	0.59 (0.72/0.91)	1.9	73
He lifetime (year)	5.0 (4.1/3.3)	1.6	—
Mass flow rate ( $\mu\text{g/s}$ )	28 (33/43)	86	3200
He tank temperature (K)	1.15	<1.50	<2.05
Film flow rate ( $\mu\text{g/s}$ )	<2	—	—

<sup>a</sup>Numbers in parenthesis are from the thermal analysis at the beginning of life and the end of life, respectively.

effect.<sup>20</sup> The SXS porous plug is made of stainless steel and has a diameter of 8.9 mm and a thickness of 6.3 mm. A hydrodynamic pore diameter or an equivalent circular opening is 3.8  $\mu\text{m}$ , while the filtration is 0.5  $\mu\text{m}$ , which means that only particles smaller than this would go through the plug. Upstream, the porous plug is attached to the helium tank as shown in Fig. 1(a).

When the superfluid helium goes through this device, it begins to evaporate due to lower pressure downstream. The latent heat of evaporation cools down liquid helium near the outside of the plug. Then, the superfluid helium conducts heat from the tank due to the nonzero size of pores. The temperature difference denoted as  $\Delta T$  is an important parameter to reduce the film flow out of the porous plug.

### 2.3 Orifice

A narrow tube called an orifice is another critical component to suppress the film flow. Even with the porous plug, the Van der Waals force leads to a film on the walls, and the mobility of superfluid gives rise to film flow. The film flow rate within a tube is limited by the smallest perimeter of the vent line. Therefore, just outside the porous plug, we placed a stainless steel tube with an inner diameter of 1.4 mm, which reduces the film flow down to  $\sim 8 \mu\text{g/s}$ .

Thermal conduction along the tube is strictly limited. If there is a heat flow from the downstream of the tube, the film flow at the downstream can recondensate, leading to a larger film loss. For this purpose, the tube has a length of 117 mm and is made of stainless steel as shown in Figs. 1(a) and 1(b). The thermal conductivity of the tube is then suppressed to  $\sim 0.01 \text{ mW/K}$  at 1.1 K. When  $\Delta T$  is 50 mK, the conductive heat would be  $\sim 0.5 \mu\text{W}$ . Since the heat to evaporate the superfluid helium of  $1 \mu\text{g/s}$  is 20  $\mu\text{W}$ , an evaporation of the film flow more than  $\sim 0.025 \mu\text{g/s}$  cannot occur with this tube.

### 2.4 Heat Exchanger

The heat exchanger has a role to evaporate the remaining film flow coming out of the tube. Because the film flow is colder than the helium tank by  $\Delta T$  as mentioned in Sec. 2.2, almost all the film will evaporate inside the heat exchanger and the latent heat cools down the tank.

The heat exchanger is made of copper for good thermal conductivity and has a hollow shape with a 54-mm diameter and

a 5-mm plate thickness. The thermal conductivity between the heat exchanger and the tank is about 50 mW/K. This allows evaporating up to  $\sim 120 \mu\text{g/s}$  of evaporation of superfluid He at 1.1 K assuming a  $\Delta T$  of 50 mK. This is an order of magnitude larger than the expected film flow out of the tube of  $\sim 8 \mu\text{g/s}$ . It has been shown experimentally that a  $\Delta T > 50 \text{ mK}$  results in no mobile film remaining after the heat exchanger and thus no loss of liquid helium.

### 2.5 Knife-Edge Devices

Finally, a pair of knife-edge devices is placed after the heat exchanger to limit the film flow in case the porous plug  $\Delta T < 50 \text{ mK}$ . Each of the knife-edge devices has sharp edges with a curvature radius of  $< 100 \text{ \AA}$ . A surface tension can suppress the film and limit the thickness of  $< 20 \text{ \AA}$ . Therefore, the edges must be atomically sharp. Also, nested edges are needed to reduce the thermal conductance across each knife-edge. The knife-edge devices can limit the film flow even if the  $\Delta T$  across the porous plug is unexpectedly small.

We fabricated the knife-edge devices from a silicon wafer by ourselves. The sharp edges were made by using anisotropic wet KOH etching of silicon (110) wafers. A central hole to vent helium gas was made with deep reactive ion etching. Each knife-edge device has a square shape of  $10 \times 10 \text{ mm}^2$  with 28 edges and  $\phi 1.5 \text{ mm}$  through a hole in the center, as shown in Fig. 1(c).

The two devices are glued on other sides of a split flange made of Invar. The thermal conductivity between the two sides must be small for the same reason as the tube. Therefore, the two sides are connected via a small tube with an inner diameter of 0.7 mm and a length of 3.6 mm. The thermal conductivity via the tube is  $\sim 0.1 \text{ mW/K}$  at 1.1 K, suppressing a recondensation of the film and a subsequent flow.

## 3 Ground Measurements

### 3.1 Setup

The FM of the SXS porous plug and film flow suppression system was tested before and after it was installed in the FM dewar. Before installation, tests were carried out in a special test apparatus. To immerse the porous plug in superfluid helium, the FM system was set at the bottom of the test helium tank so that the porous plug gets wet. For the same purpose, the tests in the FM dewar were conducted by tilting the dewar. These ground tests are described in detail by Ezoe et al.,<sup>19</sup> but we will briefly review the results and introduce an empirical model to estimate the mass flow rate from temperatures of the porous plug and the helium tank.

### 3.2 Mass Flow Rate

The helium flow rate through a porous plug is a function of the temperature of the superfluid helium and the temperature gradient  $\Delta T$  across the plug. A hysteresis in flow rate versus downstream pressure is known to exist in porous plugs in general and considered to arise by a movement of a vapor–liquid phase boundary inside the porous plug. The average phase boundary is most probably not reversible but depends on whether the flow rate is increasing or decreasing.<sup>20</sup>

Figure 2(a) shows the mass flow rate through the porous plug and film flow suppression system at fixed temperatures of the helium tank. The flow rate is higher when the tank temperature rises because of a higher vapor pressure of superfluid helium.

The flow rate increases as a function of  $\Delta T$  since higher  $\Delta T$  indicates lower pressure downstream of the porous plug.

At each tank temperature, a lower branch is when the helium flow rate is decreasing and an upper branch corresponds to when the flow rate is increasing. This behavior is similar to other porous plugs used in past space missions.<sup>20</sup> To investigate a hydrostatic head effect, data were also taken at various liquid levels. Higher liquid levels give larger flow rates because the hydrostatic head is not negligible compared to the saturated vapor pressure at low tank temperatures. Data points taken in the component level tests at the lowest liquid level are consistent with those obtained in the FM dewar tests.

At the tank temperature of 1.15 K, the mass flow rate is  $\sim 40 \mu\text{g/s}$  at  $\Delta T$  of 50 mK and higher than the requirement of  $28 \mu\text{g/s}$  by  $\sim 30\%$ . However, the saturated vapor pressure of  $^4\text{He}$  is 57 Pa at 1.15 K, while the hydrostatic head at a liquid level of 5 cm is 67 Pa. The extra hydrostatic head will decrease the measured  $\Delta T$ . This assumption was supported by the fact that a test porous plug showed  $\sim 40$  and  $\sim 30 \mu\text{g/s}$  at the liquid level of 7 and 3.5 cm, respectively. We thus concluded that this porous plug will meet the requirement.

The other two requirements were also satisfied. The flow rate at 1.50 and 2.00 K exceeds 86 and  $3200 \mu\text{g/s}$ , respectively. Even though the hydrostatic head is still not negligible at 1.50 K, where the saturated vapor pressure of  $^4\text{He}$  is 470 Pa,  $86 \mu\text{g/s}$  is satisfied with a large margin.

Based on these on-ground data, we constructed an empirical model to predict a mass flow rate  $\dot{m}$  in orbit from the helium tank temperature  $T_{\text{tank}}$  and  $\Delta T$  across the plug. The lower and the upper branches are fitted with a simple linear function:  $\dot{m}(T_{\text{tank}}, \Delta T) = A(T_{\text{tank}})\Delta T + B(T_{\text{tank}})$ .  $A$  and  $B$  can be approximated by phenomenological curves as a function of  $T_{\text{tank}}$  [At first, we tried a simple power law for the fit of the coefficients  $A$  and  $B$  but found large discrepancies. Hence, we decided to divide the temperature range below and above 1.30 K and used a polynomial function instead of a power law for  $A$  in the lower branch when  $T \geq 1.3$  K. The two coefficients are given as follows:

$$\begin{aligned}
 A &= 0.050197T_{\text{tank}}^{7.0993}, & B &= 19.526T_{\text{tank}}^{3.7595} & (\text{upper branch, } T_{\text{tank}} < 1.3 \text{ K}), \\
 A &= 0.033671T_{\text{tank}}^{4.7750}, & B &= 19.656T_{\text{tank}}^{4.3918} & (\text{lower branch, } T_{\text{tank}} < 1.3 \text{ K}), \\
 A &= 0.060408T_{\text{tank}}^{6.7078}, & B &= 7.4291T_{\text{tank}}^{7.5946} & (\text{upper branch, } T_{\text{tank}} \geq 1.3 \text{ K}), \\
 A &= 9.6543T_{\text{tank}}^2 - 24.304T_{\text{tank}} + 15.396, & B &= 9.2773T_{\text{tank}}^{7.3128} & (\text{lower branch, } T_{\text{tank}} \geq 1.3 \text{ K}).
 \end{aligned}$$

Here, we used only the lowest liquid-level data taken in the component level tests, to minimize the hydrostatic head effect.

Figure 2(b) compares the data points with model predictions. The model represents the data well with a typical error of 10% to 20%. At high tank temperatures and large  $\Delta T$  (e.g., 2.00 K and 500 mK), the error seems to become larger but such conditions were not realized in orbit. Because the hydrostatic head is minimized but is not zero, this empirical model can still overestimate the mass flow rate if we compare the model with on-orbit data. Therefore, when we compare the empirical model with the flight data in Sec. 4.1, the smaller mass flow rate model by multiplying the model result by a constant factor is tested as described later.

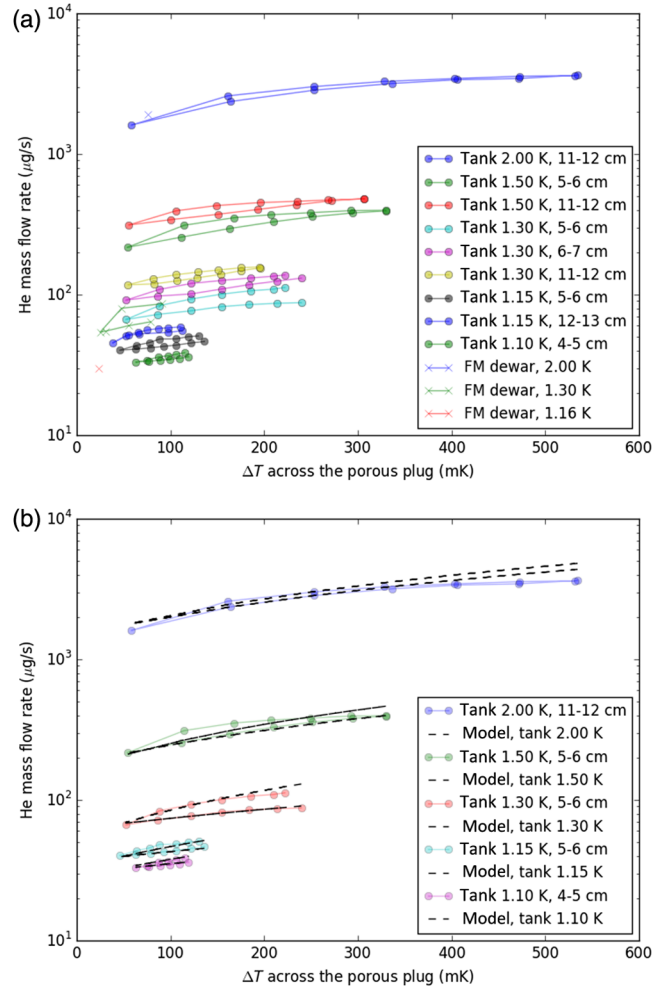


**Fig. 2** (a) Mass flow rate as a function of  $\Delta T$  across the porous plug at various helium tank temperatures and (b) the same as panel (a) but comparison with the empirical model.

### 3.3 Film Flow Rate

The film flow out of the porous plug and film flow suppression system was quantitatively measured in the component level tests. We prepared a copper test cell in the downstream of the whole system and added a heater to examine a temperature rise of the test cell.

Figure 3 shows the results. When there is a film flow coming into the test cell, the temperature rise is small. Once all the film flow evaporates, the test cell temperature rapidly rises as a function of the input heater power. This is the same method utilized in the ASTRO-E XRS and the Suzaku XRS2 experiments.<sup>14</sup>

We took data at a tank temperature of 1.15 K and two different  $\Delta T$ s (50 and 23 mK). The hydrostatic head was minimized to be 5 to 6 cm. For each data set, we fitted the temperature rise

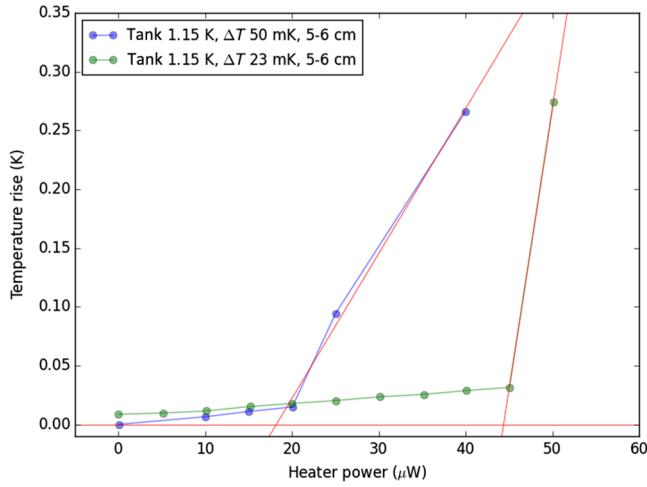


**Fig. 3** Film flow measurements. The horizontal axis represents a heater power to the test cell. The vertical axis indicates a temperature rise of the copper test cell at the downstream of the porous plug and the film flow suppression system.

with a linear function and estimated the heater power necessary to evaporate the film flow. The estimated heat power was 19 and 45  $\mu\text{W}$ , corresponding to a film flow rate of 0.9 and 2  $\mu\text{g/s}$ , respectively, assuming the latent heat of superfluid helium at this temperature. Therefore, the requirement for the film flow is satisfied even with a  $\Delta T$  of 23 mK.

### 3.4 Flow Rate Test Before Launch

One day before launch (L-1), a flow rate through the porous plug and film flow system was measured at the Tanegashima Space Center. This test was to confirm that there is no restriction in the vent line and the mechanical valve named V4 is properly closed. The valve V4 allows helium gas to bypass the porous plug and was used to quickly vent the helium tank on-ground.<sup>3</sup> Since V4 should be closed on-orbit, we closed V4 before launch and then measured the flow rate as a final check.

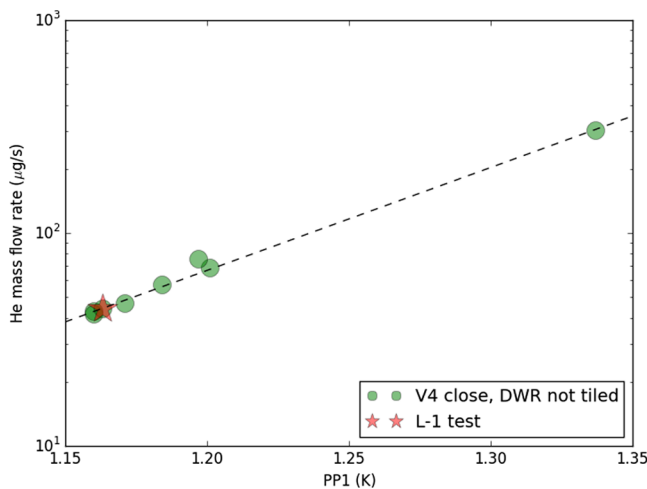


**Fig. 4** Helium gas flow rate when the bypass valve V4 is closed and the dewar is not tilted. A star indicates the data taken 1 day before launch, while circles are others taken during various on-ground tests.

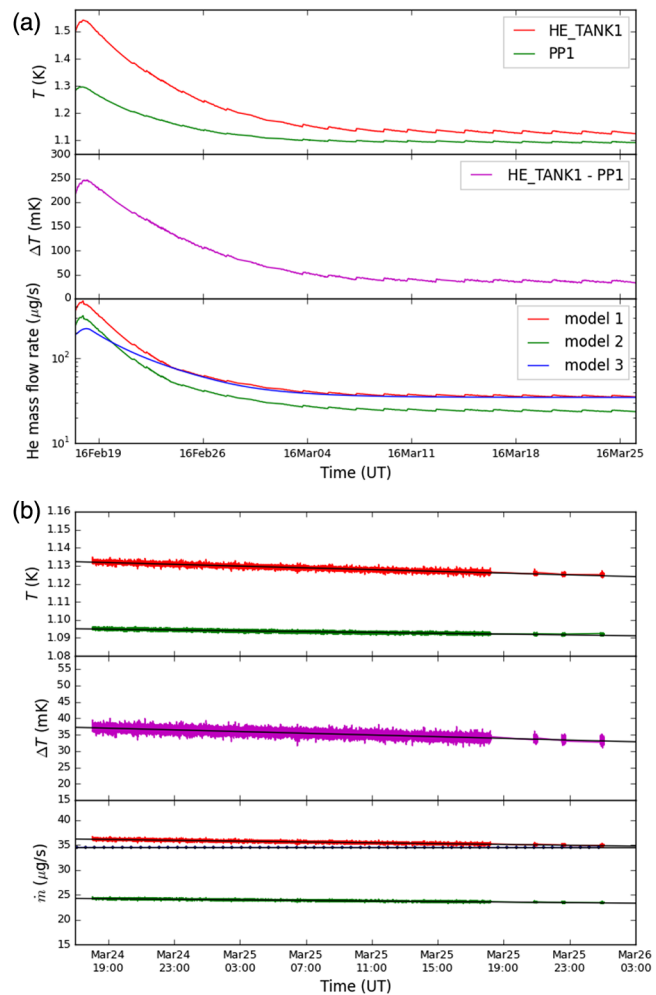
We note that the test configuration is different from the component level tests and the SXS dewar tests as described in Sec. 3.1, because the dewar was on the spacecraft and could not be tilted. However, superfluid helium can crawl up the wall, and the porous plug can be partially wet, causing a  $\Delta T$ . The flow rate does not obey the empirical model because of this difference. Therefore, we had taken the reference data in the same configuration beforehand.

Figure 4 shows the obtained data compared to those taken in the other past FM dewar tests. The flow rate is as expected from the downstream temperature of the porous plug, which is most probably due to the fact that the downstream temperature of the plug reflects a saturated vapor pressure of helium gas. After this flow rate test, we closed the helium vent valve V5 and stopped pumping on the helium tank with vacuum pumps.

## 4 In-Flight Performance

### 4.1 Temperature Profiles

Hitomi was launched on February 17, 2016, 08:45 (UT). The helium vent valve V5 was opened at 08:50. This is the first operation of the SXS after launch and was done during rocket acceleration due to a risk of the so-called castle's catastrophe,<sup>21</sup> in



**Fig. 5** (a) Temperature profiles of the helium tank and porous plug,  $\Delta T$  across the porous plug, and the estimated mass flow rate by three models and (b) the same as panel (a) but a close-up view of the last part.

which all the superfluid helium may drain off into the space. For the catastrophe to occur, there would have to be liquid helium outside the plug where it could reach a heat source. Then, the thermomechanical effect would work in reverse and pump the superfluid helium from the tank.

Figure 5(a) shows the temperature profile of the helium tank (He tank1) and the downstream temperature of the porous plug (PP1) after the vent valve was opened.  $\Delta T$  across the plug clearly exists, suggesting that the helium liquid is separated from the gas by the porous plug as designed.

All the cryocoolers were off before launch, causing a continuous temperature rise of the helium tank. We then turned on the cryocoolers step by step and the tank temperature began to decrease. After about one month, the tank temperature settled down to the thermal equilibrium temperature of  $\sim 1.12$  K. Cyclic temperature rises occur due to ADR recycles. Details on these initial operations are summarized in other papers.<sup>3,22</sup>

Estimated helium mass flow rates from the tank temperature and  $\Delta T$  across the plug are shown in the bottom of Fig. 5(a). Three curves are plotted. Model 1 corresponds to the empirical model as described in Sec. 3.2. Model 2 is  $2/3$  (67%) of the empirical model to roughly take into account the hydrostatic head effect. The tank temperature peaks around February 17, 2016, 22:40 (UT). The upper branch model was used before the peak, while the lower branch model was utilized after that. For simplicity, we did not use the upper branch model for the temperature rises due to the ADR recycles, because the time intervals are short. Model 3 is estimated from the thermal model analysis,<sup>5</sup> in order to reproduce temperature profiles of the helium tank, internal, and outer shields of the dewar.

Model 2 is closer to model 3 after launch, while model 1 fits well model 3 as the tank temperature settles down. This may indicate that the hydrostatic head effect is not a constant factor but variable depending on the tank temperature, and/or the state of the liquid and gas boundary inside the plug may be slightly different from that on the ground.

The spacecraft lost control on March 26, 2016, due to a series of attitude problems. Figure 5(b) shows a close-up of the last part of the temperature profiles. As is clear from the data, the porous plug and the film flow suppression system were working properly. The tank temperature was decreasing from 1.13 to 1.12 K, while  $\Delta T$  was from 36 to 33 mK after the ADR recycle.

The final tank temperature is consistent with our expectation but  $\Delta T$  is smaller than  $\sim 50$  mK by  $\sim 15$  mK. The ground film flow measurement suggests that the film flow rate is  $< 2 \mu\text{g/s}$  as required with this  $\Delta T$ . The estimated mass flow rates of models 1 to 3 are  $\sim 35$ , 23, and  $34 \mu\text{g/s}$ , respectively. Models 1 and 3 match and coincide with the estimated heat load to the tank of  $\sim 0.7$  mW.

## 4.2 Volume of the Superfluid Helium

Another line of evidence that the porous plug and the film flow suppression system worked properly after launch is an estimated volume of the superfluid helium in the tank. Every time the ADR recycles, the tank temperature rises and falls as a function of time as seen in Fig. 5(a). This allows a measurement of the heat capacity of the helium tank and consequently a volume of the superfluid helium inside it. This is called ADR mass gauge.<sup>4</sup>

Figure 6 shows the estimated volume compared to those by integrating the estimated mass flow rates of the three models since launch. We here assumed an initial fill of 37.0 L from on-ground estimates. Most of the ADR mass gauge data fall

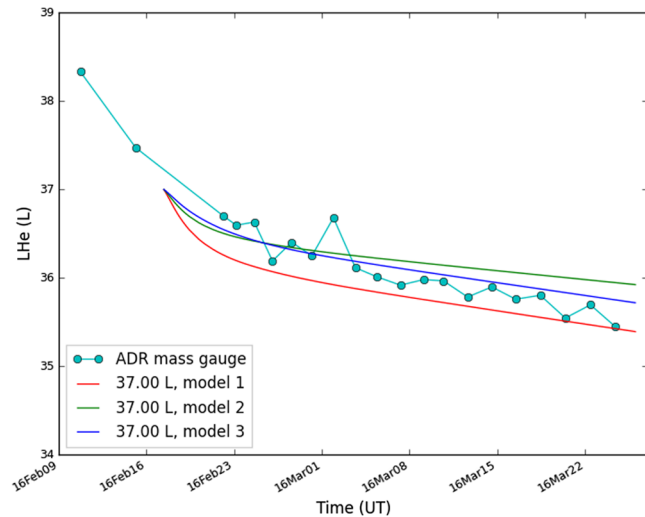


**Fig. 6** Estimated volume of the superfluid helium after launch based on the ADR mass gauging and the mass flow rate models.

between models 1 and 3. Therefore, no significant loss of helium due to the film flow (e.g., a factor of 2 or 3 as expected if there is no film flow suppression system) would exist, which suggests that the porous plug and film flow suppression system works. On the other hand, the mass loss rate inferred from the ADR mass gauge method was  $\sim 20\%$  higher than predicted based on the thermal model of the cryogenic system (model 1) or the empirical model (model 3). One possible explanation for this possible excess vent rate is that the  $\Delta T$  across the porous plug was smaller than anticipated, due for example to a higher than expected vent line impedance which may lead to an increase of the film flow, although there remains uncertainties in the estimations due to the limited lifetime of the spacecraft and also the resolution of the thermometers of the porous plug.

## 5 Conclusion

We have developed the SXS porous plug phase separator and the film flow suppression system. This was a challenge, since the mass flow rate is smaller than past space missions using the superfluid helium and also the film flow must be strictly suppressed. Taking the same approach as the ASTRO-E XRS and the Suzaku XRS2, the whole system was designed and fabricated. We tested these components using a special test apparatus as well as in the flight dewar. The empirical model of the helium mass flow rate was constructed. The data after launch suggest that the porous plug and the film flow suppression system worked.

## References

1. T. Takahashi et al., "The ASTRO-H x-ray astronomy satellite," *Proc. SPIE* **9905**, 99050U (2016).
2. R. Kelley et al., "The ASTRO-H high-resolution soft x-ray spectrometer," *Proc. SPIE* **9905**, 99050V (2016).
3. R. Fujimoto et al., "Performance of the helium dewar and cryocoolers of ASTRO-H SXS," *Proc. SPIE* **9905**, 99053S (2016).
4. P. Shirron et al., "Design and on-orbit operation of the adiabatic demagnetization refrigerator on the ASTRO-H soft x-ray spectrometer instrument," *Proc. SPIE* **9905**, 99053O (2016).
5. H. Noda et al., "Thermal analyses for initial operations of the soft x-ray spectrometer (SXS) onboard ASTRO-H," *Proc. SPIE* **9905**, 99053R (2016).

6. S. Van Dyk, M. Werner, and N. Silbermann, "Spitzer space telescope handbook," <http://irsa.ipac.caltech.edu/data/SPITZER/docs/spitzermission/missionoverview/spitzertelescopehandbook/> (2013).
7. C. Enss, *Cryogenic Particle Detectors*, Topics in Applied Physics, Springer, Berlin (2005).
8. European Space Agency, "ISO overview," [http://www.esa.int/Our\\_Activities/Space\\_Science/ISO\\_overview](http://www.esa.int/Our_Activities/Space_Science/ISO_overview) (13 August 2013).
9. J. Mester and GP-B Collaboration, "Testing Einstein in space: the gravity probe B relativity mission," in *Séminaire Poincaré*, pp. 55–61 (2006).
10. T. Nakagawa et al., "Flight performance of the AKARI cryogenic system," *Publ. Astron. Soc. Jpn.* **59**, S377–S387 (2007).
11. S. Breon et al., "The XRS low temperature cryogenic system: ground performance tests results," *Cryogenics* **39**, 677–690 (1999).
12. K. Mitsuda and R. Kelley, "The XRS system—the first cryogenic x-ray detector in orbit," *Nucl. Instrum. Methods Phys. Res. Sect. A* **436**, 212–217 (1999).
13. R. L. Kelley et al., "The Suzaku high resolution x-ray spectrometer," *Publ. Astron. Soc. Jpn.* **59**, S77–S112 (2007).
14. P. Shirron and M. DiPirro, "Suppression of superfluid film flow in the XRS helium dewar," *Adv. Cryo. Eng.* **43**, 949–956 (1998).
15. K. Ishikawa et al., "Porous plug and superfluid helium film flow suppressor for the soft x-ray spectrometer onboard Astro-H," *Cryogenics* **50**, 507–511 (2010).
16. H. Yamaguchi et al., "Development of porous plug phase separator and superfluid film flow suppression system for the soft x-ray spectrometer (SXS) on board ASTRO-H," in *Proc. ICEC*, pp. 725–730 (2011).
17. Y. Ezoe et al., "Development of porous plug phase separator and superfluid film flow suppression system for the soft x-ray spectrometer onboard ASTRO-H," *Cryogenics* **52**, 178–182 (2012).
18. I. Mitsuishi et al., "He flow rate measurements on the engineering model for the Astro-H soft x-ray spectrometer dewar," *Cryogenics* **64**, 189–193 (2014).
19. Y. Ezoe et al., "Flight model measurements of the porous plug and film flow suppression system for the Astro-H soft x-ray spectrometer dewar," *Cryogenics* **74**, 17–23 (2016).
20. M. Murakami et al., "Experimental study on porous-plug phase separator for superfluid helium," ISAS Report, Vol. **612**, pp. 1–35, Institute of Space and Astronautical Science (1984).
21. S. Castle and M. DiPirro, "The fountain effect in aerospace cryogenics," *Adv. Cryo. Eng.* **35**, 211–221 (1990).
22. M. Tsujimoto et al., "In-orbit operation of the ASTRO-H SXS," *Proc. SPIE* **9905**, 99050Y (2016).

**Yuichiro Ezoe** is an associate professor at Tokyo Metropolitan University. He received his BS, MS, and PhD degrees in physics from the University of Tokyo in 1999, 2001, and 2004, respectively. His current research interests include x-ray microcalorimeters, x-ray telescopes, and high-energy astrophysical phenomena associated with solar system objects, massive star-forming regions, and supermassive black holes.

Biographies for the other authors are not available.